ELSEVIER

Catalysis Today 82 (2003) 207–211

CATALYSIS TODAY

www.elsevier.com/locate/cattod

Electrochemical behavior of $Ln_{0.6}Sr_{0.4}Co_{0.2}Fe_{0.8}O_{3-\delta}$ (Ln = Ce, Gd, Sm, Dy) materials used as cathode of IT-SOFC

Jianfeng Gao, Xingqin Liu, Dingkun Peng, Guangyao Meng*

The Department of Materials Science and Engineering, University of Science and Technology of China, Anhui, Hefei 230026, China

Abstract

The perovskite-type compounds $Ln_{0.6}Sr_{0.4}Co_{0.2}Fe_{0.8}O_{3-\delta}$ (Ln = Ce, Sm, Gd, Dy) used as the cathodes of intermediate temperature solid oxide fuel cell (IT-SOFC) were studied. The cells consisted of anode supported Sm-doped-ceria electrolyte bi-layer and cathode with $0.65\,cm^2$ effective area. Open-circuit voltage (OCV), *V–I* and *P–I* curves of the cells were measured over a temperature range from 400 to 800 °C, using H_2–3%H_2O as fuel and air as oxidant. Polarization potential of electrodes were measured with asymmetry three-electrode method during cell discharging. The results indicated that, Dy-SCF material cathode behaved with high catalytic activity for oxygen dissociation at low temperatures. For each cell with a particular cathode, there was a transition temperature, at which OCV of the cell reached the highest value. When temperature was higher than the transition temperature, OCV of the cell increases with decreasing temperature, whereas as temperature was lower than that, OCV decreased with lowering temperature.

Keywords: IT-SOFC; Perovskite; Cathode; Oxygen dissociation catalytic activity

1. Introduction

Reducing the cost of solid oxide fuel cells (SOFCs) is the goal currently pursued by the developers of the world. This had led to the development of intermediate temperature SOFC (IT-SOFC) operating at 500–750 °C. However, the performance of IT-SOFC is strongly influenced by the electrochemical properties of cathode since the cathode/electrolyte interface resistance increases rapidly as temperature decreases [1]. The development of high performance cathode at low temperature is in dire need.

A desired cathode material for IT-SOFC should have high electronic and oxide ionic conductivities, good compatibility with electrolyte and long-term stability, and behave with high catalytic activity for oxygen reduction. The perovskite-type $Ln_{1-x}Sr_xCo_{1-y}Fe_yO_{3-\delta}$ (LSCF) compositions (Ln respects lanthanide element) exhibit high ionic and electronic conductivity [2–5], as well as high catalytic activity for oxygen reduction even at reduced temperature [6–14]. They are considered to be more promising candidates for IT-SOFC cathode.

This work focuses on the electrochemical behaviors of the perovskite-type materials $Ln_{0.6}Sr_{0.4}Co_{0.2}Fe_{0.8}O_{3-\delta}$ (Ln = Ce, Sm, Gd, Dy) used as IT-SOFC cathode. Open-circuit voltage (OCV), *V–I* curve, *P–I* curve of cells and cathode overpotential measured

---

* Corresponding author. Tel.: +86-551-3603234; fax: +86-551-3607627.
E-mail address: mgym@ustc.edu.cn (G. Meng).

0920-5861/$ – see front matter © 2003 Elsevier B.V. All rights reserved.
doi:10.1016/S0920-5861(03)00234-7

with asymmetry three-electrode method are examined over the temperature range from 400 to 800 °C, using H_2–3%H_2O as fuel and air as oxidant.

2. Experimental

The high surface starting powders of perovskite-type compounds $Ln_{0.6}Sr_{0.4}Co_{0.2}Fe_{0.8}O_{3-\delta}$ (Ln = Ce, Sm, Gd, Dy) were synthesized by glycine-nitrate-process (GNP) [15]. They were noted as Ce-SCF, Sm-SCF, Gd-SCF and Dy-SCF, respectively. Samaria-doped-ceria $Sm_{0.2}Ce_{0.8}O_2$ (SDC) electrolyte was prepared by homogeneous co-precipitation technique with urea as precipitation reagent. The green dual phases anode consisted of 61% NiO and 39% SDC. Anode support and electrolyte bi-layer disks were prepared by uniaxially co-pressing in a die (15 mm in diameter) at a load of 230 MPa, and then sintered at 1400 °C in air for 5 h. The paste of cathode materials was coated on the surface of electrolyte side by screen printing, fired at 1150 °C in air for 1.5–3 h.

Fig. 1 shows the schematic configuration of tested cells. Testing cell was held in an intentionally built sample holder that fitted in a tube furnace. Pt mesh (80 mesh) attached on the top of cathode as a current collector and Pt wire as terminal. To keep the collector and cathode in good contact, a spring was used to press the Pt mesh collector onto cathode via an alumina disk with gas channels. Pt reference electrode was attached on the same side of cathode, a few millimeters (more than 20 times of the electrolyte layer thickness) away from the cathode. Prior to cell testing, the anode was in situ reduced with fuel gas (H_2–3%H_2O) for a few hours. Electrochemical measurements were carried out over a temperature range from 400 to 800 °C in step of 50 °C, using H_2–3%H_2O as fuel and air as oxidant. Cathode overpotential was in situ (e.g. during cell discharging) measured by a multi-meter (hp HEWLETT PACKARD 34401A). OCV of cells, *I–V* and *P–I* curves were recorded by in-home made system consisted of an interface, an electronic rheostat and a personal computer. At each step, constant temperature was kept for at least two hours to ensure that thermal equilibrium was reached. After testing, the samples were fractured for scanning electron microscopy (SEM, HITCHI, X-650) observation.

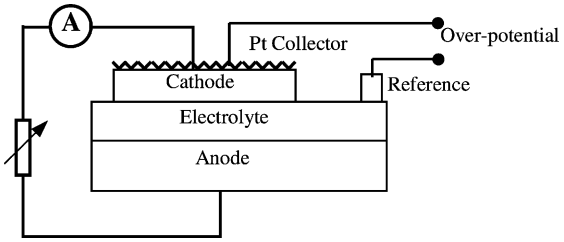

Fig. 1. The schematic configuration of tested cells.

3. Results and discussion

All the tested cells were fractured after about 140 h testing operation and the sections were observed by SEM. Fig. 2 shows the typical (SEM) view of PEN structure of tested cells. About 50 μm thick porous cathode with homogeneous microstructure were well adhered on the dense electrolyte film (90–100 μm in thickness) supported on ∼1 mm thick Ni-SDC cermet anode. For all the cathodes (Ce-SCF, Sm-SCF, Gd-SCF and Dy-SCF), no reaction between cathode and electrolyte had been observed. It is consistent with the previous report [16].

Fig. 3 shows the temperature dependence of OCV of the cells. It can be seen that OCV of every tested cell is lower than the theoretical value calculated by Nernst equation [17,18], particularly at low temperature. There is a transition temperature for each cell with particular cathode, at which OCV reaches a maximum value. As temperature is higher than the transition temperature, OCV increases with temperature decreasing. The trend is consistent with that expected by thermodynamics. When temperature is

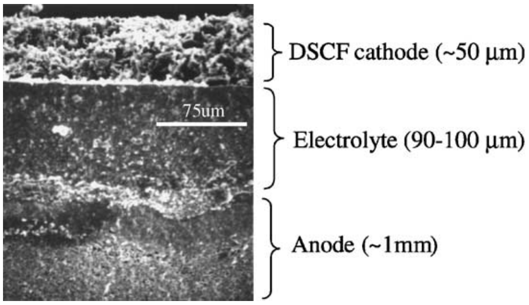

Fig. 2. The typical (SEM) section view of PEN.

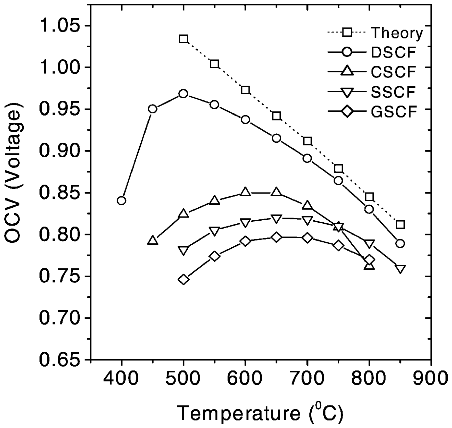

Fig. 3. Temperature dependence of OCV of cells with different cathode.

lower than the transition temperature, OCV decreases with temperature dropping, negatively deviates from the theoretic. The cells with Dy-SCF cathode showed a distinctly lower transition temperature (∼500 °C) than the others.

That OCV of cells was lower than Nernst equation's value can be likely contributed to the electronic leakage of SDC electrolyte. However, that is not the whole cause noticing that OCV of cells with Sm-SCF, Gd-SCF or Ce-SCF cathode were lower not only than the theoretic but also than that of the cell with Dy-SCF cathode. On the other hand, all the cells consisted of the same electrolyte and anode. Therefore, OCV varying with cathode, even under the same operation condition, should be rationally attributed to different catalytic activities for oxygen dissociation of the cathodes.

Oxygen reduction in the cathode of SOFC is much similar to a multiphase catalysis reaction. For instance, the elementary steps in mixed conductor cathode may include [19,20]: (i) diffusion of O_2 in gas phase to the surface of porous cathode; (ii) dissociation of chemisorbed oxygen molecule into atomic oxygen at active site; (iii) surface diffusion of oxygen atom to active site; (iv) charge transfer; (v) diffusion of O^{2-} through the cathode layer, across cathode/electrolyte interface and into electrolyte layer. The rate-determining step may be any one step. At high temperatures, such as higher than 800 °C, charger transfer is possibly the rate-determining step, whereas at lower temperatures, the rate-determining step is more possibly the dissociation of oxygen molecules into atomic oxygen [21].

The processes of oxygen chemi-adsorption and dissociation can be described as follows:

$$O_2(\text{gas}) \underset{k_a^*}{\overset{k_a}{\rightleftarrows}} O_2^*(\text{ad}) \underset{k_d^*}{\overset{k_d}{\rightleftarrows}} 2O(\text{ad}) \quad (1)$$

where k_a is the rate constant of adsorption of the incident O_2 molecule into the precursor state $O_2^*(\text{ad})$, k_a^* the rate constant of desorption of the precursor state $O_2^*(\text{ad})$, k_d the rate constant of dissociation of $O_2^*(\text{ad})$ into atomic oxygen O_{ad}, k_d^* the rate constant of recombination of chemisorbed oxygen atom.

When the processes are in equilibrium, the cathode potential (φ) is described as

$$\varphi = \frac{RT}{4F} \ln p_{O_2} + \text{constant} \quad (2)$$

where p_{O_2} is the oxygen partial pressure on the cathode, R, T, F have their usual meanings. However, as the oxygen dissociation deviates from equilibrium, the cathode potential (φ) is no more given by Eq. (2), but by

$$\varphi = \frac{RT}{4F} \ln(p_{O_2})^{\alpha} + \text{constant} \quad (3a)$$

or

$$\varphi = \frac{RT}{2F} \ln a_0 + \text{constant} \quad (3b)$$

where α is a coefficient indicating the non-equilibrium degree of oxygen dissociation from $O_2^*(\text{ad})$ into atomic oxygen O_{ad}, $\alpha \leq 1$. When the oxygen dissociation reaction is in equilibrium, $\alpha = 1$, otherwise, $\alpha < 1$; a_0 means the activity of atomic oxygen on the cathode surface, $a_0^2 = (p_{O_2})^{\alpha}$.

Therefore, it was different activity for oxygen dissociation into atoms of the cathodes that led to different cathodic potential and resulted in OCV varying with cathode even under the same condition.

By comparison, Dy-SCF cathode material showed relatively higher catalytic activity for oxygen dissociation. The cause likely rises from different Ln-cation in A-site because the four tested cathode materials Dy-SCF, Ce-SCF, Gd-SCF and Sm-SCF contain the same B-site cations and the same Sr-dopant concentration in A-site. Comparing the radii of Ce^{3+}, Sm^{3+}, Gd^{3+} and Dy^{3+}, 1.034, 0.964, 0.938 and 0.908 (Å),

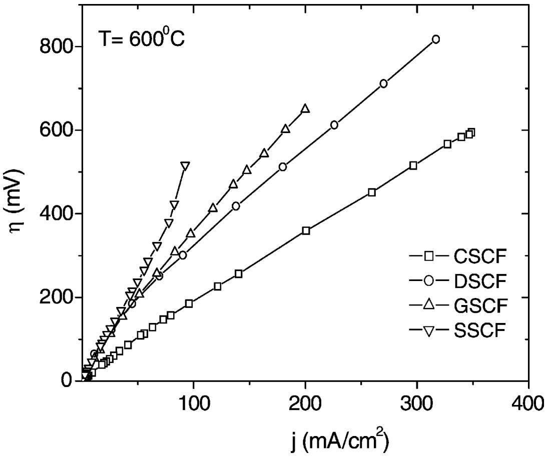

Fig. 4. Cathode overpotential vs. discharging current density of cell at 600 °C, with H_2–3%H_2O as fuel air as oxidant.

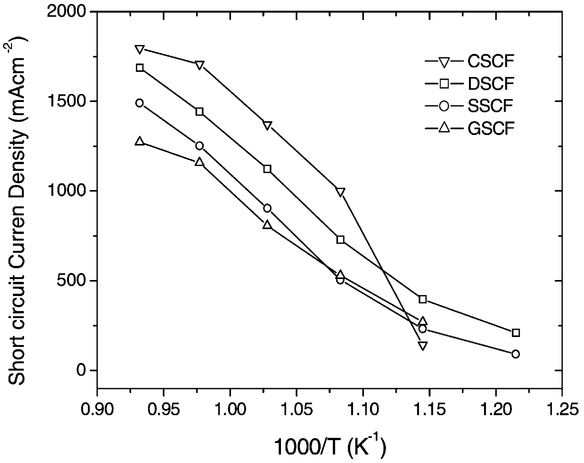

Fig. 5. Short-circuit current density of cells with different cathode.

respectively, it can be clearly seen that Dy^{3+} has the smallest radius. Assuming the average radius ($\bar{R}_A$) in A-site follows the weighted average rule, Dy-SCF has the smallest $\bar{R}_A$. According to the result by Cherry et al. [22] that smaller A-site cations and larger B-site cations clearly leads to lower oxygen migration energies in the perovskite, Dy-SCF has the lowest oxygen vacancy migration energy among them. Lower migration energy of oxygen ion (oxygen vacancy) made for oxygen vacancies diffusion from the bulk into the surface layer, particularly at relatively lower temperatures. High oxygen vacancy concentration in the surface layer improved oxygen molecule $O_2^*(ad)$ dissociation into atomic oxygen O_{ad} and resulted in a higher cathode potential (Eq. (3b)), which corresponded to higher OCV of the cell. It should be pointed that, more detailed understanding about the above-mentioned phenomena need further investigation. In this experiment, OCV of each tested cell, under a given operation condition, remained almost stable in the period of about 140 h testing (OCV–time curves were not recorded in this study).

With respect to cathode overpotential, as shown in Fig. 4, Ce-SCF has the lowest resistance for oxygen reduction reaction, the next is Dy-SCF cathode, then Gd-SCF and Sm-SCF. At 600 °C, with 100 mA/cm^2 discharging current density through the cells, the overall overpotential of the Ce-SCF cathode was 188 mV. For Dy-SCF, Gd-SCF and Sm-SCF cathode, it was 326, 360 and 567 mV, respectively. Cathode overpotential is closely related with not only the rate of oxygen dissociation, but also the transport speed of oxygen ions through cathode bulk and across cathode/electrolyte interface. The common cerium ions contained both in Ce-SCF cathode and SDC electrolyte made improvement of the contact between the cathode and the electrolyte and resulted in low Ce-SCF/SDC interface resistance. On the other hand, the catalysis of $Ce^{3+} \Leftrightarrow Ce^{4+}$ redox cycle also played a great role in oxygen reduction reaction [21,23].

Fig. 5 shows short-circuit current density of the cells at different temperatures. At high temperatures (≥600 °C), the cell with Ce-SCF cathode showed distinctly higher short-circuit current density than the others. This is consistent with the low resistance of Ce-SCF/SDC interface. However, at temperature lower than 550 °C, the cell with Dy-SCF cathode showed the largest short-circuit current. It implies that Dy-SCF has higher activity for oxygen reduction at lower temperatures, consistent with the above result of OCV variation with temperature.

4. Conclusions

$Ln_{0.6}Sr_{0.4}Co_{0.2}Fe_{0.8}O_{3-\delta}$ (Ln = Ce, Sm, Gd, Dy) compounds are successfully prepared by GNP method. The electrochemical behaviors of these materials used as SOFC cathode have been examined. All the compounds have a good chemical compatibility with Sm-doped CeO_2 electrolyte. After near a week operation at 500–850 °C, there were no obvious reaction between cathode and electrolyte.

At high temperatures, the catalysis of $Ce^{3+} \Leftrightarrow Ce^{4+}$ redox cycle plays a great role in oxygen reduction reaction. At lower temperature, the cathode material $Dy_{0.6}Sr_{0.4}Co_{0.2}Fe_{0.8}O_{3-\delta}$ (Dy-SCF) showed higher catalytic activity for oxygen dissociation. The result implied that Dy-SCF would be a better choice for the cathode material of IT-SOFC.

Acknowledgements

This work was financially supported by National Natural Science Foundation of China (contract No. 20071029) and the Ministry of Science and Technology of China (contract No. G200026409, and 2001AA323090).

References

[1] M.T. Colomer, B.C.H. Steele, J.A. Kilner, Solid State Ionics 147 (2002) 41.
[2] R.A. Lane, et al., Solid State Ionics 106 (1998) 175.
[3] B.C.H. Steele, et al., Solid State Ionics 106 (1998) 255.
[4] J.A. Lane, et al., Solid State Ionics 121 (1999) 201.
[5] N.E. Trofimenko, H. Ullmann, J. Eur. Ceram. Soc. 20 (2000) 1241.
[6] A. Mineshige, et al., J. Solid State Chem. 142 (1999) 374.
[7] S.B. Adler, Solid State Ionics 111 (1998) 125.
[8] M.H.R. Lankhorst, et al., Solid State Ionics 96 (1997) 21.
[9] M.H.R. Lankhorst, et al., J. Electrochem. Soc. 144 (1997) 1261.
[10] M.H.R. Lankhorst, et al., J. Electrochem. Soc. 144 (1997) 1268.
[11] F.M. Figueiredo, et al., Solid State Ionics 111 (1998) 273.
[12] W. Zipprich, et al., Solid State Ionics 101–103 (1997) 1015.
[13] T. Kawada, et al., Solid State Ionics 121 (1999) 271.
[14] R.A. De Souza, J.A. Kilner, Solid State Ionics 126 (1999) 153.
[15] L.A. Chick, et al., Mater. Lett. 10 (1–2) (1990) 6.
[16] B.C.H. Steele, K. Zheng, R.A. Rudkin, N. Kiriazis, M. Christie, in: M. Dokiya, O. Yamamoto, H. Tagawa, S.C. Singhal (Eds.), Proceedings of the Fourth International Symposium on Solid Oxide Fuel Cells, The Electrochemical Society, Yokohama, Japan, 1995, p. 1028.
[17] S.W. Zha, C.R. Xia, G.Y. Meng, J. Appl. Electrochem. 31 (2001) 93.
[18] T. Kudo, H. Obayashi, J. Electrochem. Soc. 123 (1976) 415.
[19] A. Mitterdorfer, L.J. Gauckler, Solid State Ionics 120 (1999) 211.
[20] H. Uchida, et al., J. Electrochem. Soc. 146 (1) (1999) 11.
[21] Y. Takeda, et al., J. Electrochem. Soc. 134 (1987) 2656.
[22] M. Cherry, M.S. Islam, C.R.A. Catlow, J. Solid State Chem. 118 (1995) 125.
[23] T.X.T. Sayle, S.C. Parker, C.R.A. Catlow, Surf. Sci. 316 (1994) 329.